Benchmarking chemistry-climate models' 9.6-μm ozone band top-of-atmosphere (TOA) flux using instantaneous radiative kernels (IRK) products

Le Kuai[1], Kevin W. Bowman[2], Helen Worden[3], Susan Kulawik[4], Dejian Fu[2], Vivienne Payne[2], Kazu. Miyazaki[5], and CCMI committees

1. University of California, Los Angeles; 2. Jet Propulsion Laboratory, California Institute of Technology; 3. National Center for Atmospheric Research; 4. Bay Area Environmental Research Institute; 5. Japan Agency for Marine-Earth Science and Technology, Japan

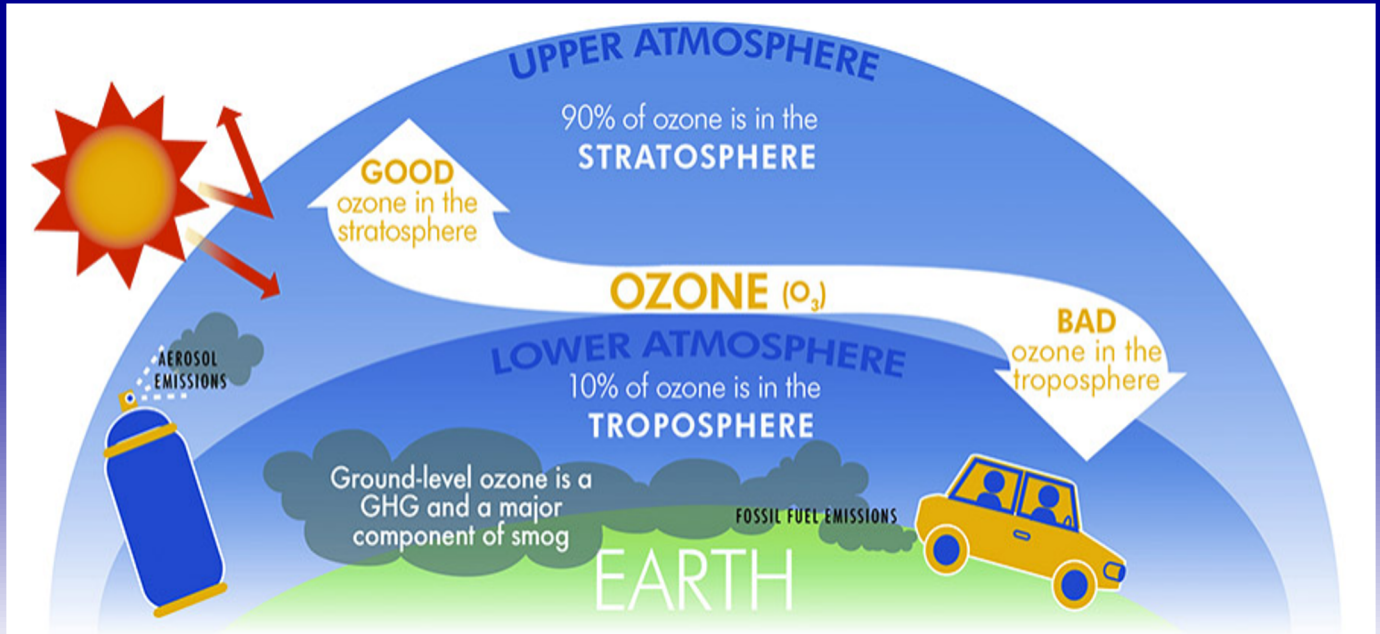

© The Field Museum, ECCo., 2012

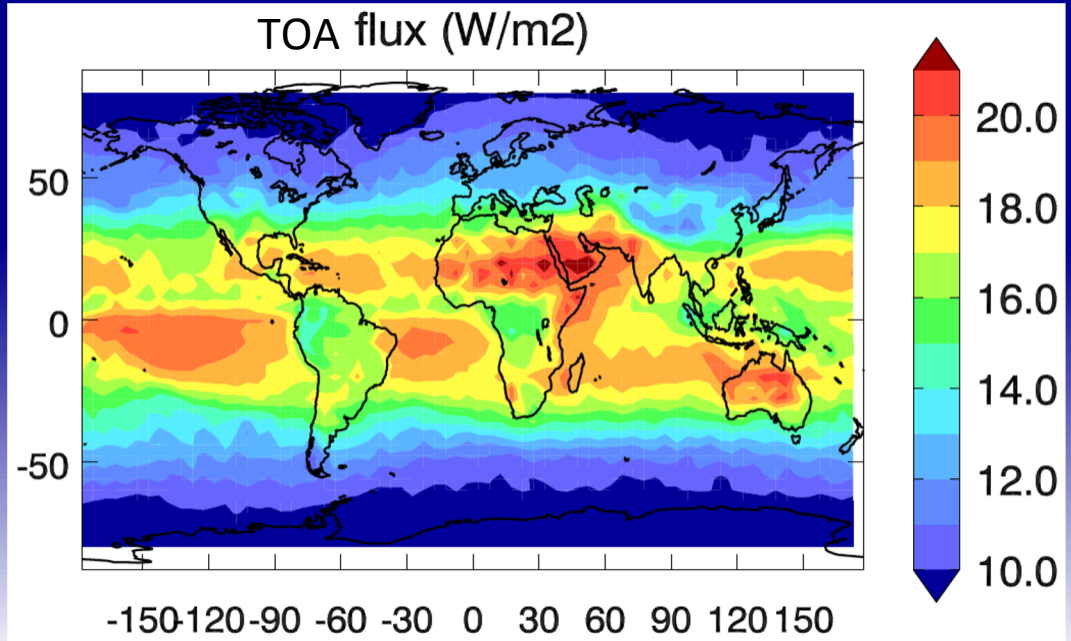

Tropospheric O_3 Radiative Forcing & 9.6 µm O_3 band

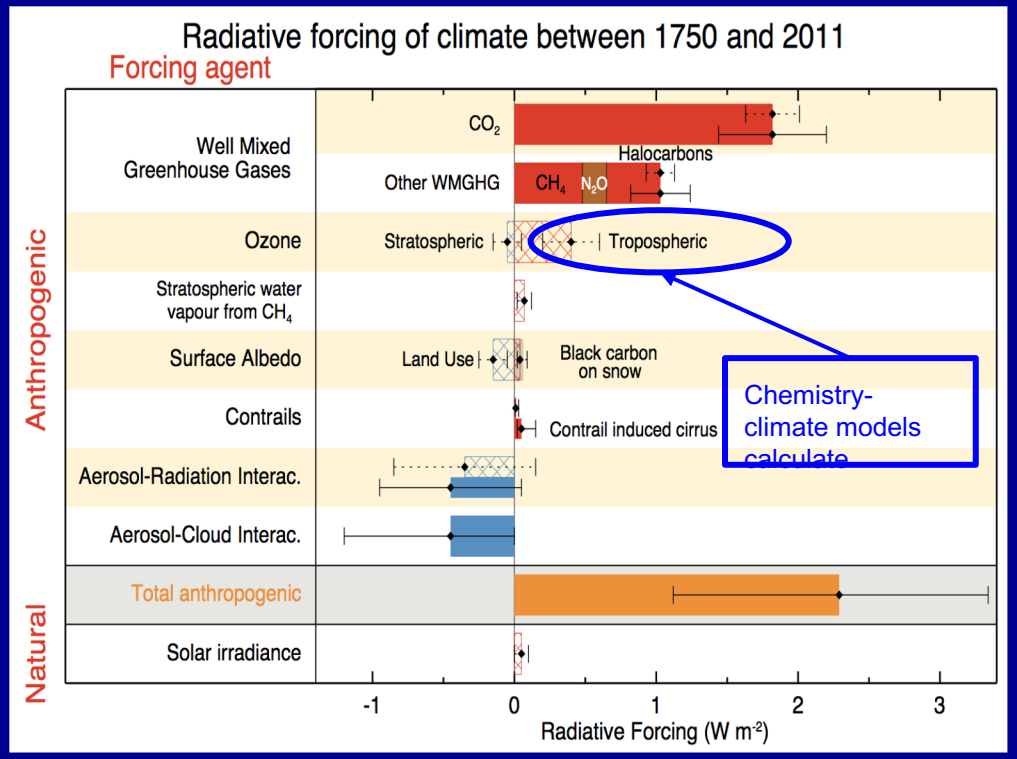

IPCC AR5, 2013

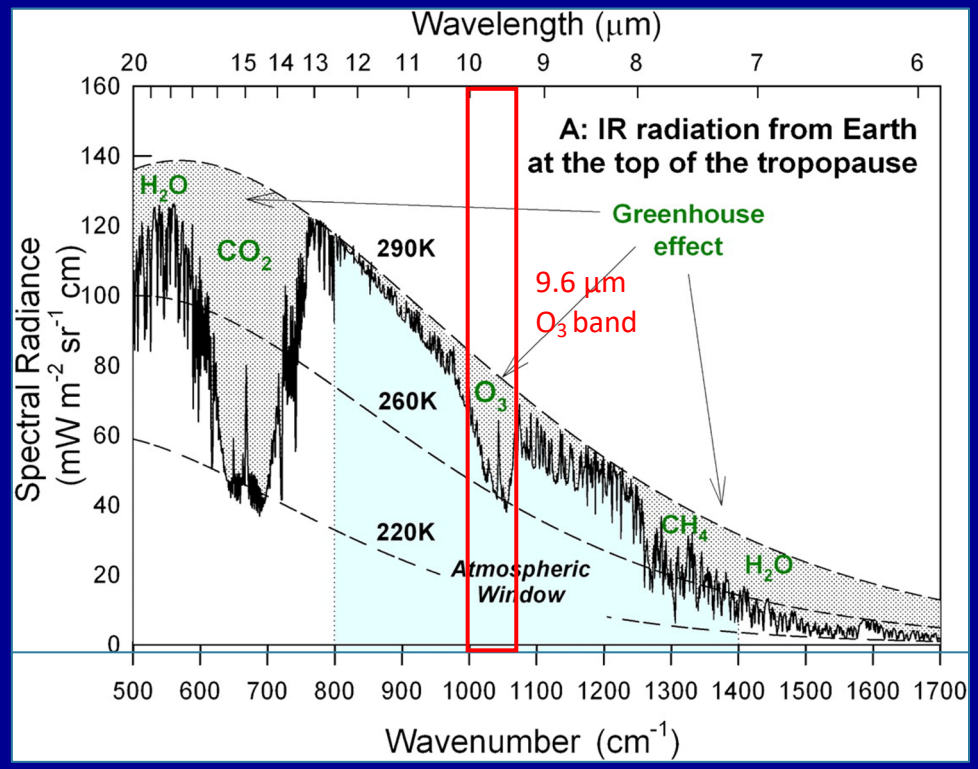

Wallington T J et al. PNAS 2010;107:E178-E179

- Tropospheric ozone (O_3) is a GHG.
- Increases in tropospheric O_3 from pre-industrial to present day add radiative forcing (RF) to the climate.
- The chemical-climate model estimated radiative forcing (RF) range widely from +0.2 to +0.6 Wm^{-2}.
- ~80% of tropospheric O_3 RF is in longwave (rest is shortwave).
- 97% of the O_3 longwave absorption is in the 9.6 µm band [Rothman et al., 1987].

Motivations:

- TES, IASI, AIRS, CrIS and models provides 9.6-µm O_3 band flux and flux sensitivity (e.g. IRK, LWRE)
- O_3 GHG effect is more unevenly distributed than long-lived GHG gases,
- Ozone LWRE depends on temperature, relative humidity via atmospheric opacity (Kuai et al., 2017)
- How do modeled TOA fluxes compare to the observations?
- Biases in model O_3, water vapor, and temperature are sources of uncertainties in O_3 RF.
- Benchmarking present day ozone band flux is the first step to understand model divergence in ozone forcing.
- Comparison of IRK between model and observations also understands the sources of uncertainties in O_3 RF

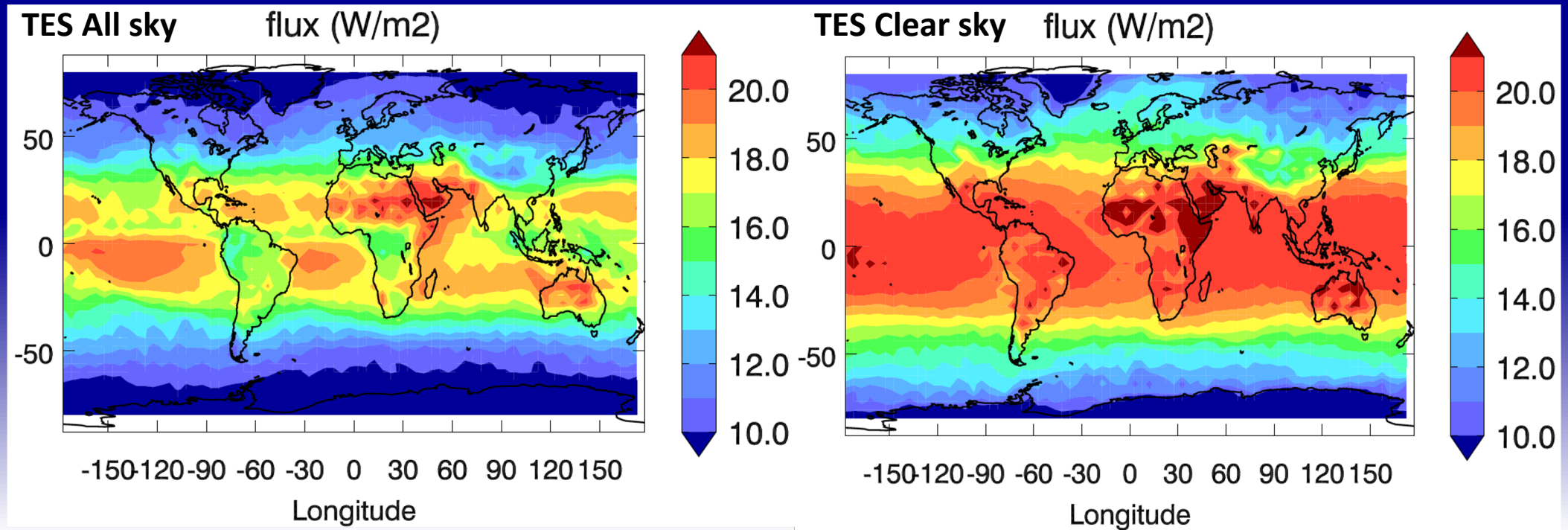

IRK Relevant Products

TES:

Worden et al., 2011
Aghedo et al., 2011
Bowman et al., 2013
Kuai et al., 2017

IASI:

Doniki et al., ACP, 2015

- Ozone Band TOA Flux (W/m^2)
- IRK (e.g. W/m^2/ppb)
- Tropospheric O_3 longwave radiative effect (LWRE, W/m^2)

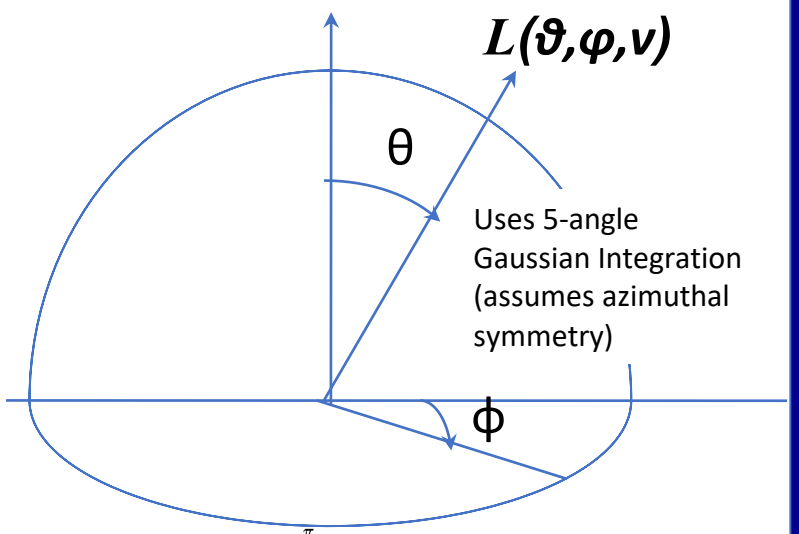

$$F_{TOA} = \int dv \int_0^{2\pi} \int_0^{\frac{\pi}{2}} L_v(\theta)\cos\theta\sin\theta\, d\theta\, d\phi$$

$$IRK = \frac{\partial F_{TOA}}{\partial q_l}$$

q_l: O_3, H_2O, T_a, *etc.*

$$LWRE = \Delta F_{TOA} = \sum_{l=surface}^{tropopause} \left(\frac{\partial F_{TOA}}{\partial q_l}\right) q_l$$

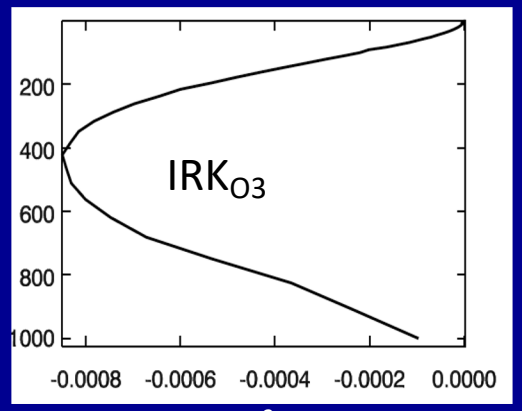

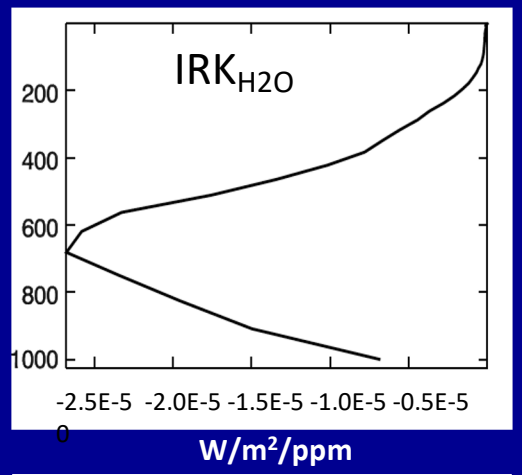

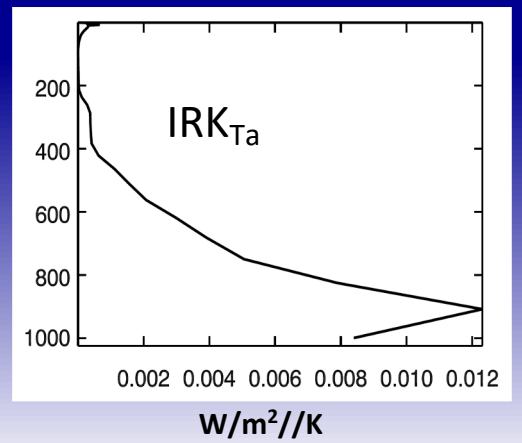

Extend TES Record With AIRS and Other Instruments

	TES	AIRS	IASI	CrIS
Satellite Altitude (km)	705	705	817	832
Spectral resolution (cm^{-1})	0.06	0.4~0.6	0.25	0.625
Viewing mode	Nadir only	0°~49.5°	0°~48.3°	0°~48.33°

Extend TES Record With AIRS and Other Instruments

	TES	AIRS	IASI	CrIS
Satellite Altitude (km)	705	705	817	832
Spectral resolution (cm^{-1})	0.06	0.4~0.6	0.25	0.625
Viewing mode	Nadir only	0°~49.5°	0°~48.3°	0°~48.33°

Gaussian Integration Nadir Angles

GI Nadir Angle	Weighting	TES & AIRS	IASI	CrIS
1	0.015748	63.6765	61.2563	61.5613
2	0.073909	59.0983	57.0576	57.3154
3	0.146387	48.1689	46.7816	46.9590
4	0.167175	32.5555	31.7557	31.8588
5	0.096782	14.5752	14.2483	14.2906

Extend TES Record With AIRS and Other Instruments

- Spectral resolution may not matter
- But micro-window gaps seem critical
- Reconstruct the simulation in gaps are necessary.

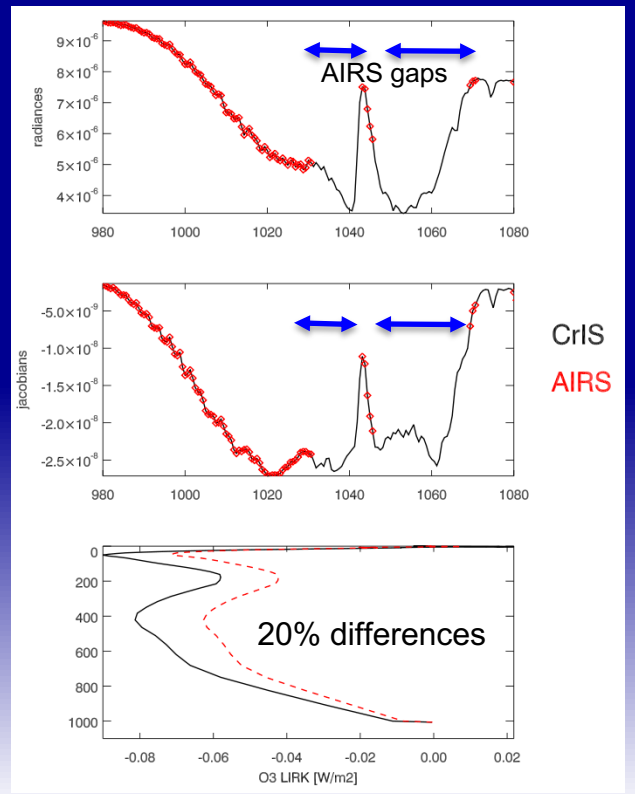

	TES	AIRS	IASI	CrIS
Satellite Altitude (km)	705	705	817	832
Spectral resolution (cm^{-1})	0.06	0.4~0.6	0.25	0.625
Viewing mode	Nadir only	0°~49.5°	0°~48.3°	0°~48.33°

Gaussian Integration Nadir Angles

GI Nadir Angle	Weighting	TES & AIRS	IASI	CrIS
1	0.015748	63.6765	61.2563	61.5613
2	0.073909	59.0983	57.0576	57.3154
3	0.146387	48.1689	46.7816	46.9590
4	0.167175	32.5555	31.7557	31.8588
5	0.096782	14.5752	14.2483	14.2906

Extend TES Record With AIRS and Other Instruments

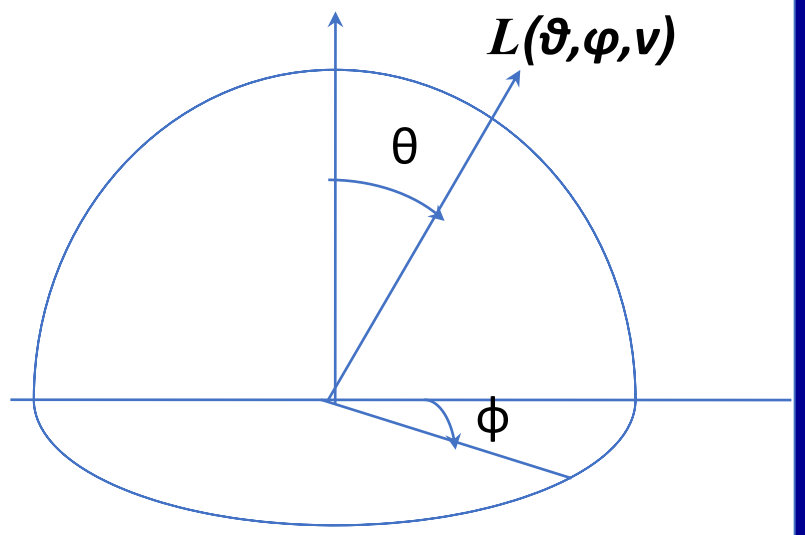

Values of off-nadir scan

- Provide off-nadir radiances

	TES	AIRS	IASI	CrIS
Satellite Altitude (km)	705	705	817	832
Spectral resolution (cm^{-1})	0.06	0.4~0.6	0.25	0.625
Viewing mode	Nadir only	0°~49.5°	0°~48.3°	0°~48.33°

Gaussian Integration Nadir Angles

GI Nadir Angle	Weighting	TES & AIRS	IASI	CrIS
1	0.015748	63.6765	61.2563	61.5613
2	0.073909	59.0983	57.0576	57.3154
3	0.146387	48.1689	46.7816	46.9590
4	0.167175	32.5555	31.7557	31.8588
5	0.096782	14.5752	14.2483	14.2906

Extend TES Record With AIRS and Other Instruments

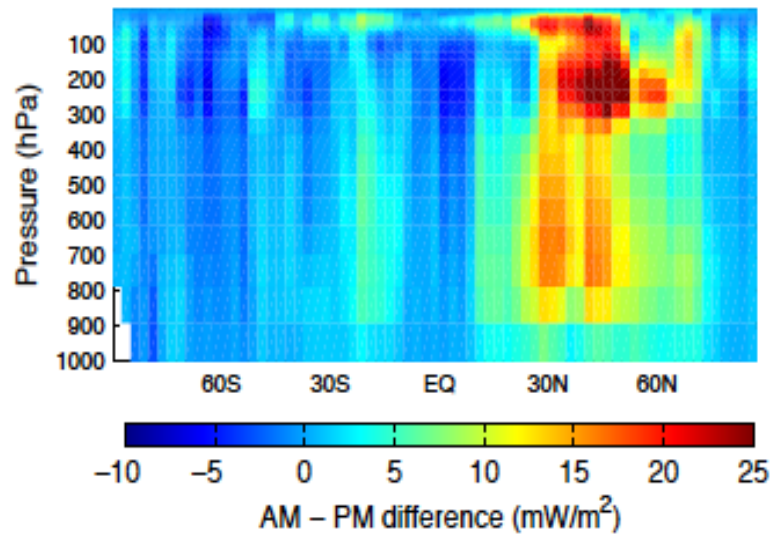

(S. Doniki et al., 2015)

Values of off-nadir scan

- Provide off-nadir radiances
- Global bi-daily data
- Morning and evening observations

	TES	AIRS	IASI	CrIS
Satellite Altitude (km)	705	705	817	832
Spectral resolution (cm^{-1})	0.06	0.4~0.6	0.25	0.625
Viewing mode	Nadir only	0°~49.5°	0°~48.3°	0°~48.33°

Gaussian Integration Nadir Angles

GI Nadir Angle	Weighting	TES & AIRS	IASI	CrIS
1	0.015748	63.6765	61.2563	61.5613
2	0.073909	59.0983	57.0576	57.3154
3	0.146387	48.1689	46.7816	46.9590
4	0.167175	32.5555	31.7557	31.8588
5	0.096782	14.5752	14.2483	14.2906

Global IRKs FOR O_3, H_2O, and T

- The bias at the regions with large IRKs would contribute more errors to the flux than other places.
- All kernels are large over low latitudes and decrease to high latitude.

- The TOA flux is most sensitive to
  - tropical lower troposphere for temperature (~900 hPa) & water vapor (~700 hPa)
  - Tropical mid-tropospheric O_3 (~400 hPa)

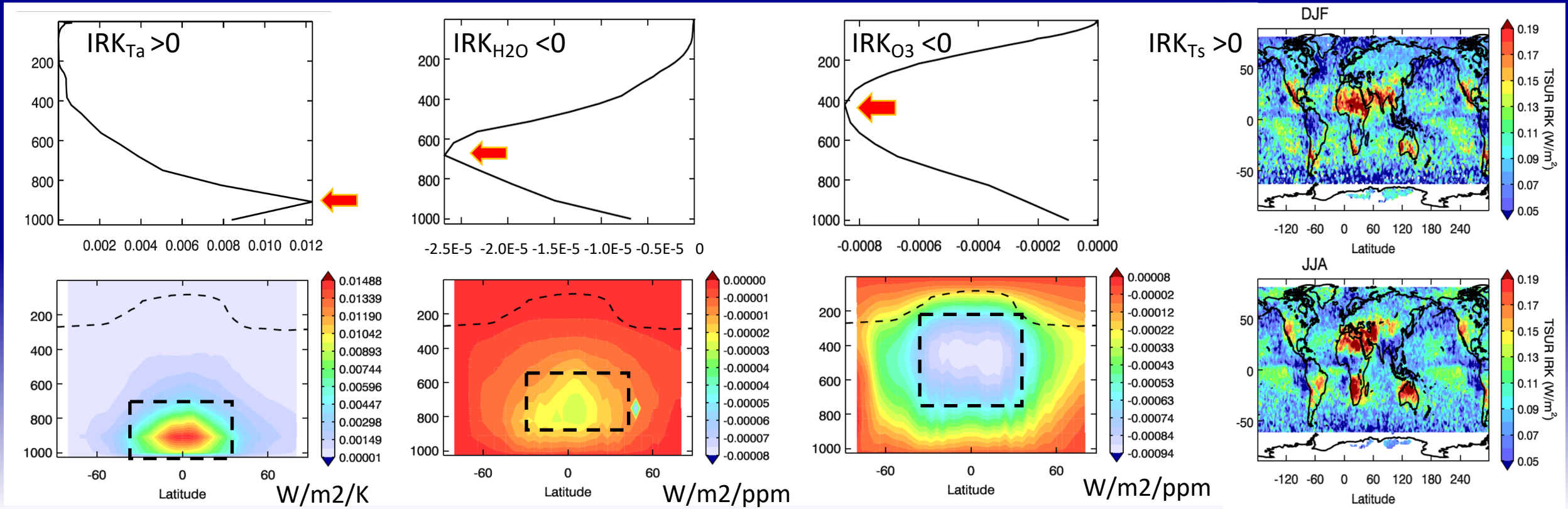

A FUNDAMENTAL EQUATION:

$$\underbrace{\Delta F_{TOA}}_{\text{9.6 µm band flux change}} = \underbrace{\frac{\partial F_{TOA}}{\partial O_3}\Delta O_3}_{O_3} + \underbrace{\frac{\partial F_{TOA}}{\partial T_{sur}}\Delta T_{sur}}_{\text{Surface temperature}} + \underbrace{\frac{\partial F_{TOA}}{\partial T_{atm}}\Delta T_{atm}}_{\text{Atmos. temperature}} + \underbrace{\frac{\partial F_{TOA}}{\partial H_2O}\Delta H_2O}_{\text{Water vapor}} + \underbrace{r_s}_{\text{residual}}$$

A FUNDAMENTAL EQUATION:

Instantaneous Radiative Kernel (IRK): $\frac{\partial F_{TOA}}{\partial q}$ e.g. $\frac{\partial F_{TOA}}{\partial O_3}$

$$\underbrace{\Delta F_{TOA}}_{\text{9.6 µm band flux change}} = \underbrace{\frac{\partial F_{TOA}}{\partial O_3}\Delta O_3}_{O_3} + \underbrace{\frac{\partial F_{TOA}}{\partial T_{sur}}\Delta T_{sur}}_{\text{Surface temperature}} + \underbrace{\frac{\partial F_{TOA}}{\partial T_{atm}}\Delta T_{atm}}_{\text{Atmos. temperature}} + \underbrace{\frac{\partial F_{TOA}}{\partial H_2O}\Delta H_2O}_{\text{Water vapor}} + \underbrace{r_s}_{\text{residual}}$$

APPLICATION: TOA flux bias attribution

What controls ΔF_{TOA}:
- TOA flux geo-temporal variation

S. Doniki et al., 2015

Instantaneous Radiative Kernel (IRK): $\frac{\partial F_{TOA}}{\partial q}$ e.g. $\frac{\partial F_{TOA}}{\partial O_3}$

$$\underbrace{\Delta F_{TOA}}_{\text{9.6 µm band flux change}} = \underbrace{\frac{\partial F_{TOA}}{\partial O_3}\Delta O_3}_{O_3} + \underbrace{\frac{\partial F_{TOA}}{\partial T_{sur}}\Delta T_{sur}}_{\text{Surface temperature}} + \underbrace{\frac{\partial F_{TOA}}{\partial T_{atm}}\Delta T_{atm}}_{\text{Atmos. temperature}} + \underbrace{\frac{\partial F_{TOA}}{\partial H_2O}\Delta H_2O}_{\text{Water vapor}} + \underbrace{r_s}_{\text{residual}}$$

APPLICATION: TOA flux bias attribution

What controls ΔF_{TOA}:

- TOA flux geo-temporal variation
- Model bias to observations:

e.g. TOA flux bias:

$$\Delta F_{TOA} = F_{TOA}^{MOD} - F_{TOA}^{OBS}$$

Instantaneous Radiative Kernel (IRK): $\frac{\partial F_{TOA}}{\partial q}$ e.g. $\frac{\partial F_{TOA}}{\partial O_3}$

$$\underbrace{\Delta F_{TOA}}_{\text{9.6 µm bai flux change}} = \underbrace{\frac{\partial F_{TOA}}{\partial O_3}\Delta O_3}_{O_3} + \underbrace{\frac{\partial F_{TOA}}{\partial T_{sur}}\Delta T_{sur}}_{\text{Surface temperature}} + \underbrace{\frac{\partial F_{TOA}}{\partial T_{atm}}\Delta T_{atm}}_{\text{Atmos. temperature}} + \underbrace{\frac{\partial F_{TOA}}{\partial H_2O}\Delta H_2O}_{\text{Water vapor}} + \underbrace{r_s}_{\text{residual}}$$

$$\Delta O_3 = O_3^{MOD} - O_3^{OBS}$$

$$\Delta T_{sur} = T_{sur}^{MOD} - T_{sur}^{OBS}$$

Chemistry-Climate Model Initiative (CCMI):

		Model	CCMI runs		
1	CCCma	CMAM	refC1	r1i1p1	v1
2	ETH-PMOD	SOCOL3	refC1	r1i1p1	v1
3	GSFC	GEOSCCM	refC1	r1i1p1	v1
4	MESSy	EMAC-L47MA	refC1	r1i1p1	v1
5	MESSy	EMAC-L90MA	refC1	r1i1p1	v1
6	MRI	MRI-ESM1r1	refC1	r1i1p1	v1
7	GFDL/NOAA	AM3	-	-	-
8	NCAR	CESM	-	-	-
	Reanalysis	ERA-Interim	-	-	-

- Model inter-comparison exercises
- After ACCMIP
- Coordinate existing and future model comparison and evaluation
- Associate modeling activities
- In support of the upcoming IPCC

refC1:

- uses state-of-knowledge historic forcing
- observed sea surface conditions
- the models simulate the recent past (1960–2010).
- The models are free-running

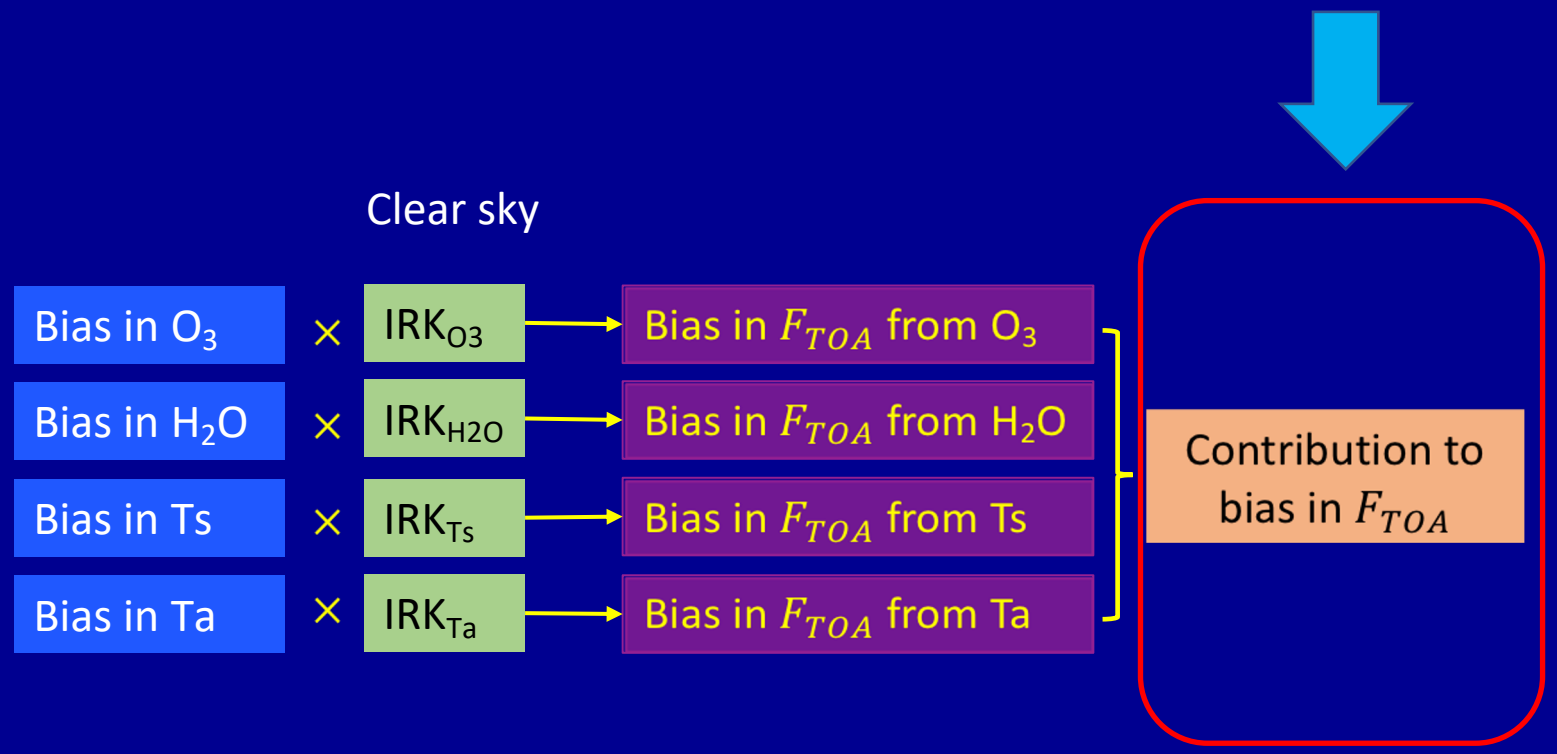
Clear sky
Bias in O_3
×
IRK_{O3}
Bias in F_{TOA} from O_3
Bias in H_2O
×
IRK_{H2O}
Bias in F_{TOA} from H_2O
Bias in Ts
×
IRK_{Ts}
Bias in F_{TOA} from Ts
Bias in Ta
×
IRK_{Ta}
Bias in F_{TOA} from Ta
Contribution to bias in F_{TOA}

TOA FLUX BIAS:
Significantly different between models

$$\Delta F_{TOA} = \sum_i \Delta F_{TOA}^{var_i}$$

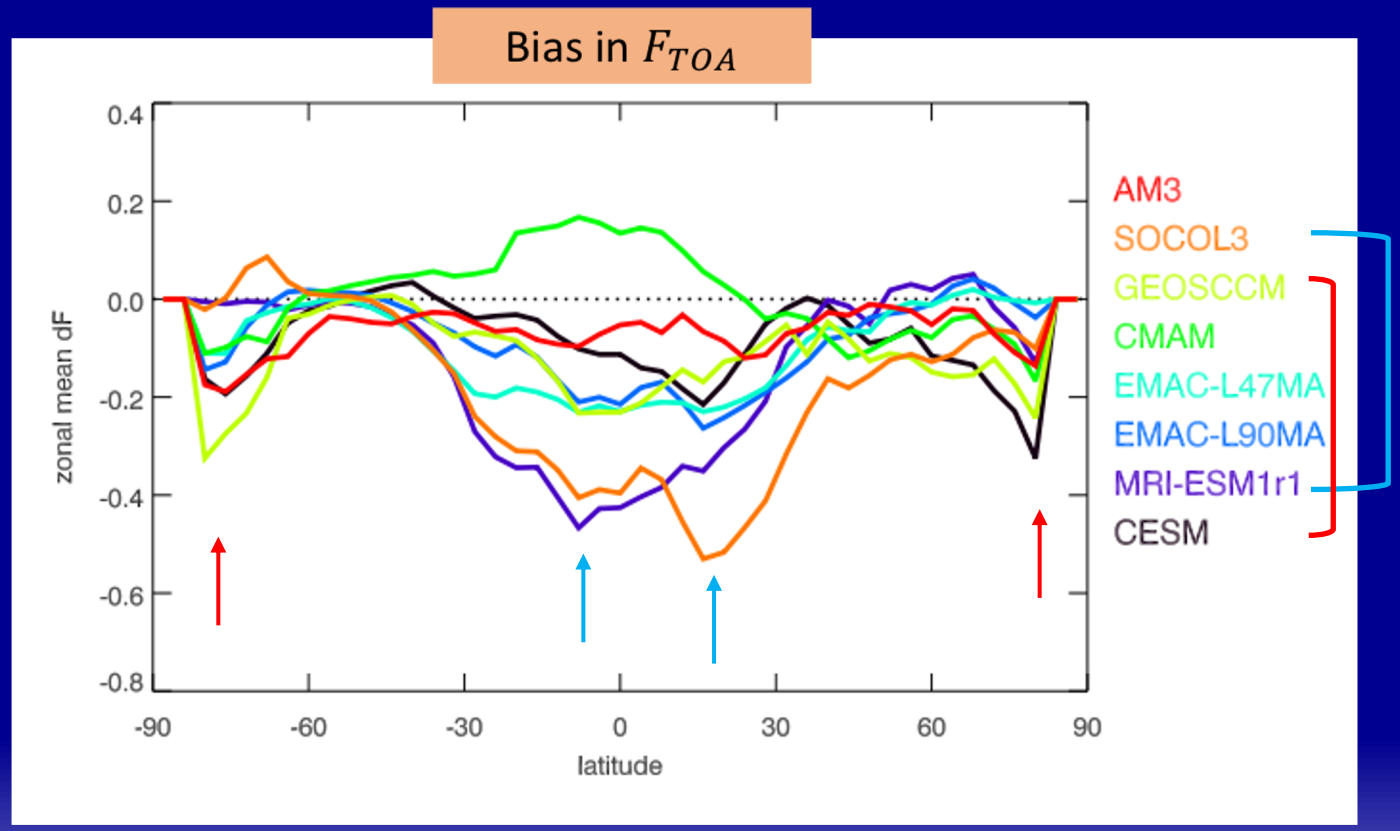

- Major biases in tropics and subtropics for most models.
  - Tropics: large negative bias except CMAM (positive bias).
  - SOCOL3 and MRI-EMS1r1 both have the largest negative biases (-0.4 to -0.6 W/m^2) between ±30°.
- Secondary peaks at polar regions, e.g. GEOSCCM and CESM

Implications:

- Model's atmospheres are more opaque than reanalysis atmosphere at 9.6 micron ozone band
- On average of 0.2 W/m^2 less emitted to the TOA.
- A opaque atmosphere will have a weaker IRK than transparent atmosphere.

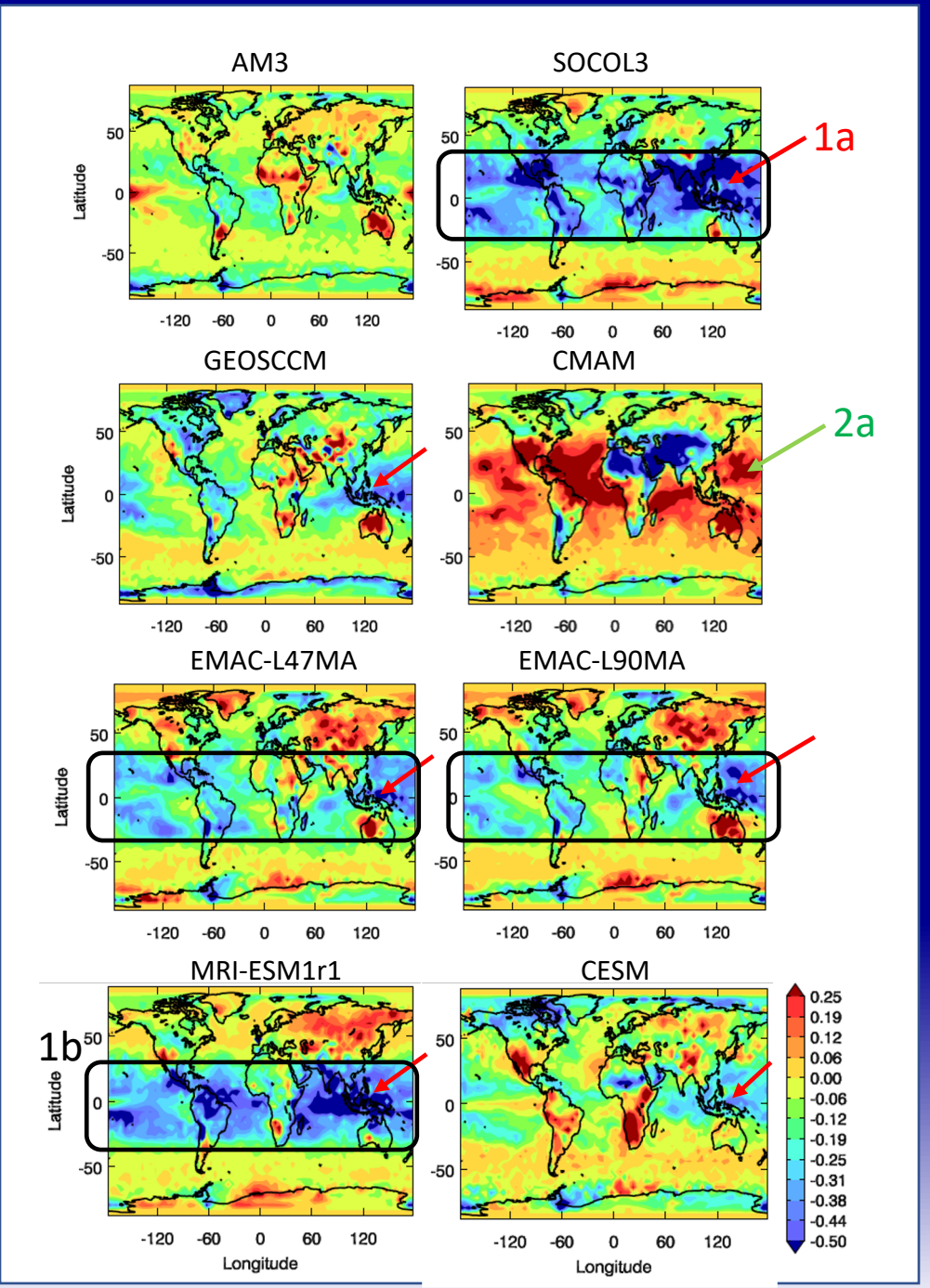

F_{TOA} BIAS: Expand To A Global View

1. SOCOL3, 2 EMAC, and MRI-ESM1r1 biased low at:
   a. the Indonesia warm pool region
   b. subtropical ocean
   c. ⇒ tropical negative biases in zonal flux
2. CMAM
   a. strong overestimates (-0.25 W/m2) over ocean
   b. ⇒ tropical positive biases in zonal flux
   c. N. Africa, Middle East and Asia biased low.
   d. ⇒ less overestimate than SH subtropics

Attribution

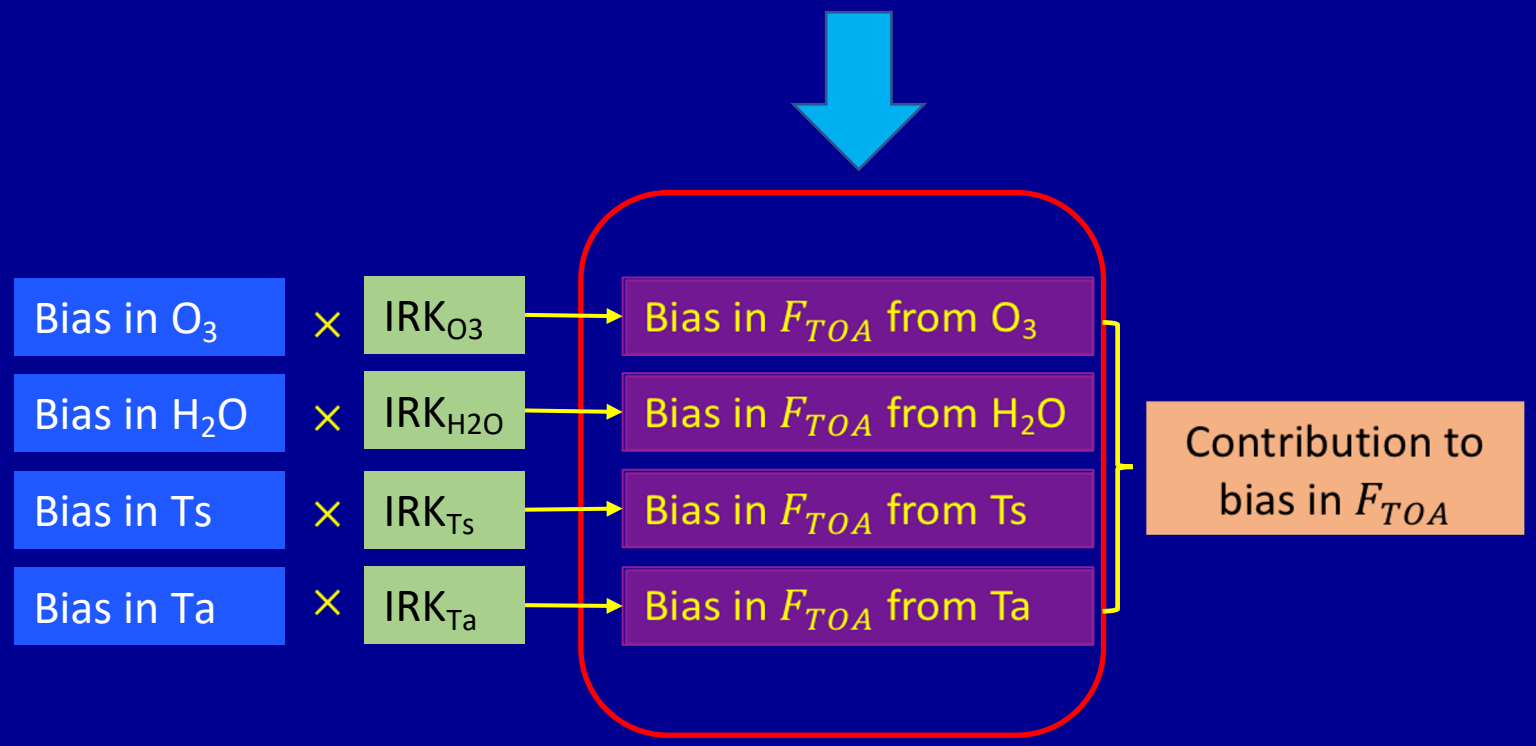

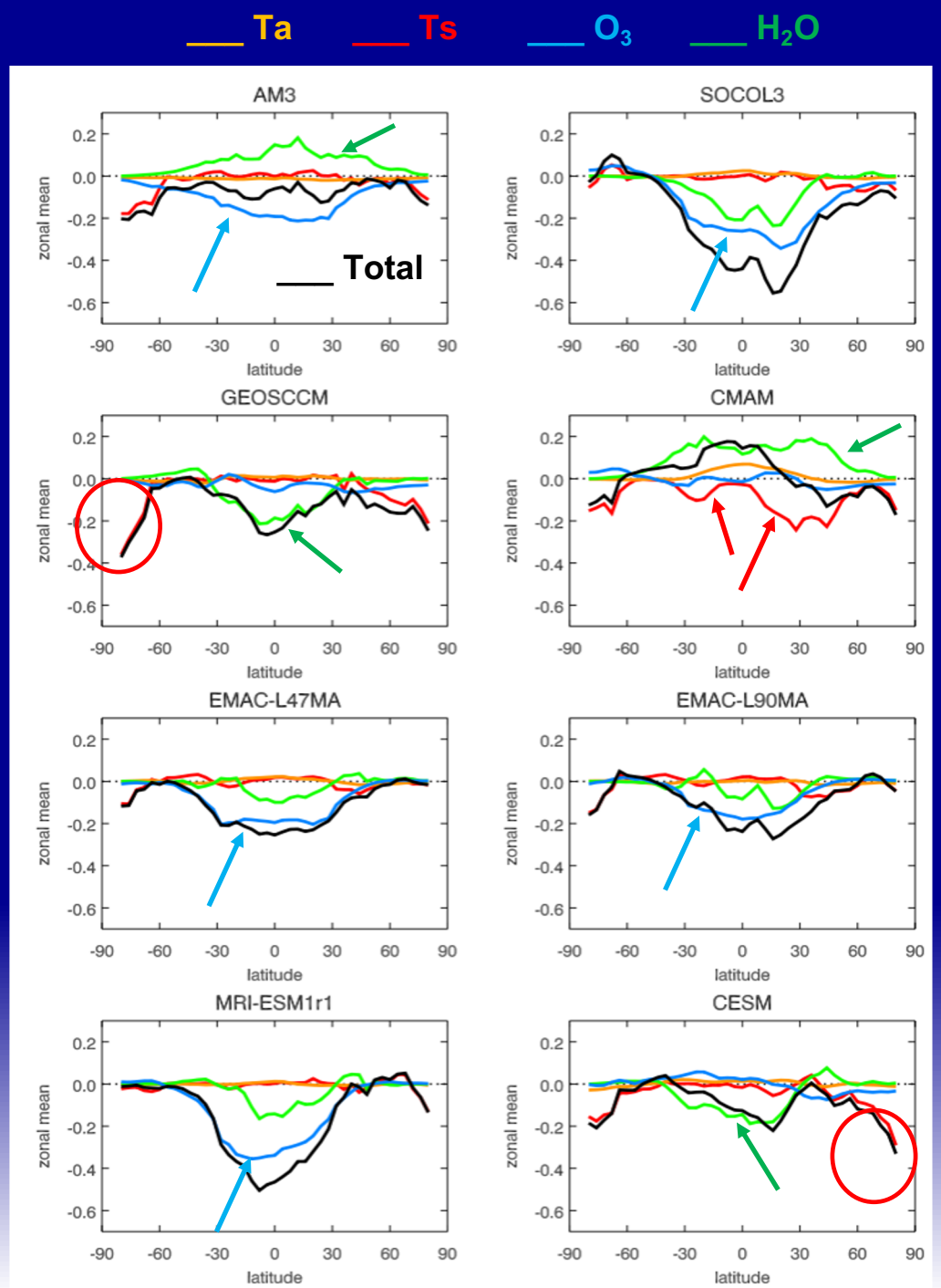

Flux bias attribution:

- Ta: Generally small contributions for most models.
- Ts: commonly small contributions except
  - CMAM (large negative bias (-0.2 to -0.3 W/m2) in both subtropics) and polar region
  - Polar bias ⇒ flux bias: GEOSCCM, CESM (-0.3 W/m2).
- O_3 contributes to low latitudes
  - Strong and dominant in SOCOL3 and MRI-ESM1r1 at (-0.2 to -0.4 W/m2);
  - moderate in AM3 and both EMAC runs (-0.2 W/m2);
  - weaker in GEOSCCM, CMAM, and CESM.
- H_2O contribution mainly in low latitudes as O_3
  - Moderate in magnitude (~0.2 W/m^2) compare to O_3
  - AM3: biased high and balanced by biased low from O_3
  - AM3 has right answers for the wrong reasons.
  - CMAM: also bias high and partly balanced by biased low from Ts over both subtropics but not tropics.
  - Dominant sources for total bias in GEOSCCM and CESM

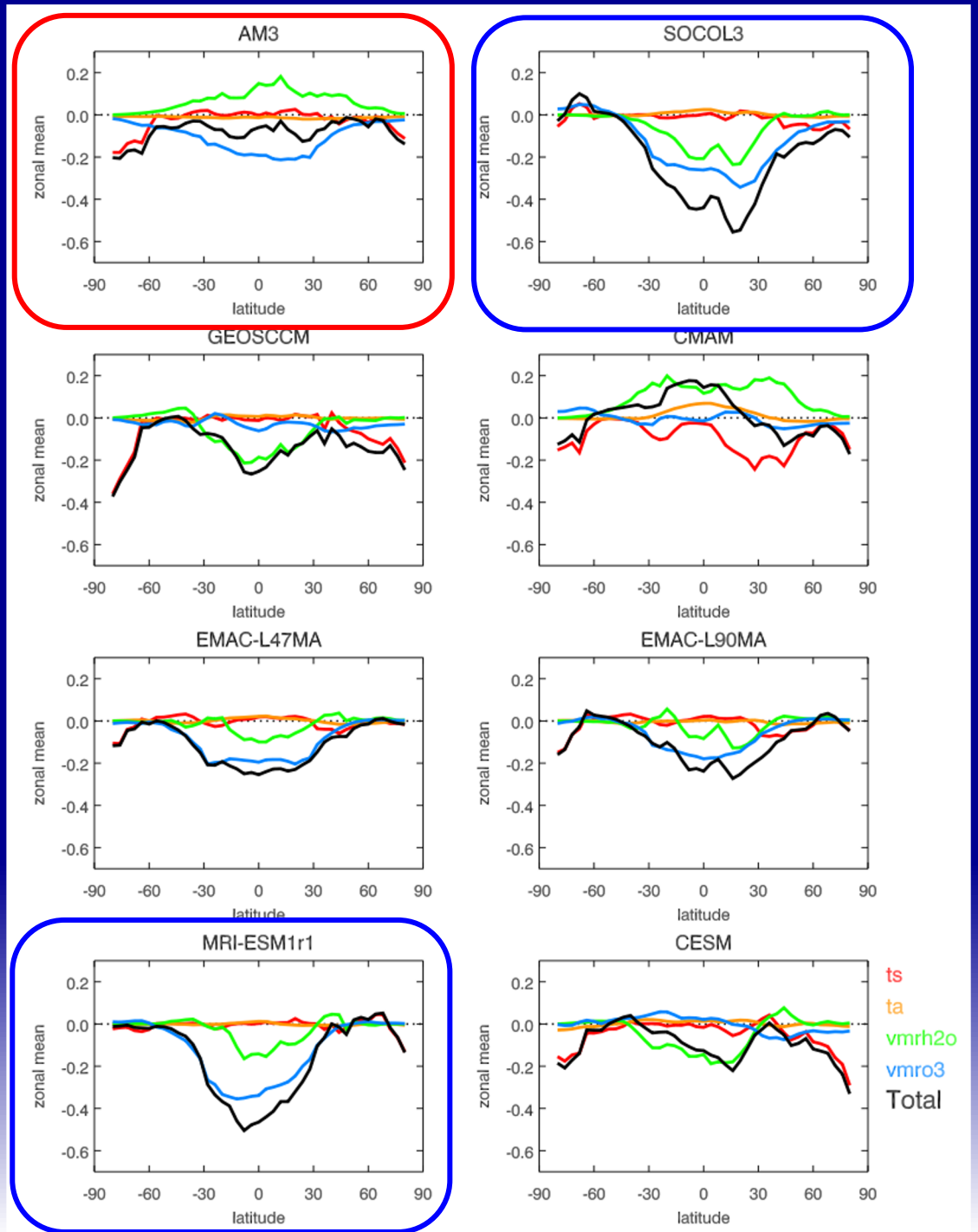

Flux bias attribution:

Model	Contribution rank			
	1	2	3	4
AM3	O3	H2O	Ts	Ta
SOCOL3	O3	H2O	Ts	Ta
GEOSCCM	Ts	H2O	O3	Ta
CMAM	Ts/Ts	H2O	O3	Ta
EMAC-L47MA	O3	H2O	Ts	Ta
EMAC-L90MA	O3	H2O	Ts	Ta
MRI-ESM1r1	O3	H2O	Ts	Ta
CESM	H2O	Ts	O3	Ta

Polar region large
Tropical region large
Small contribution

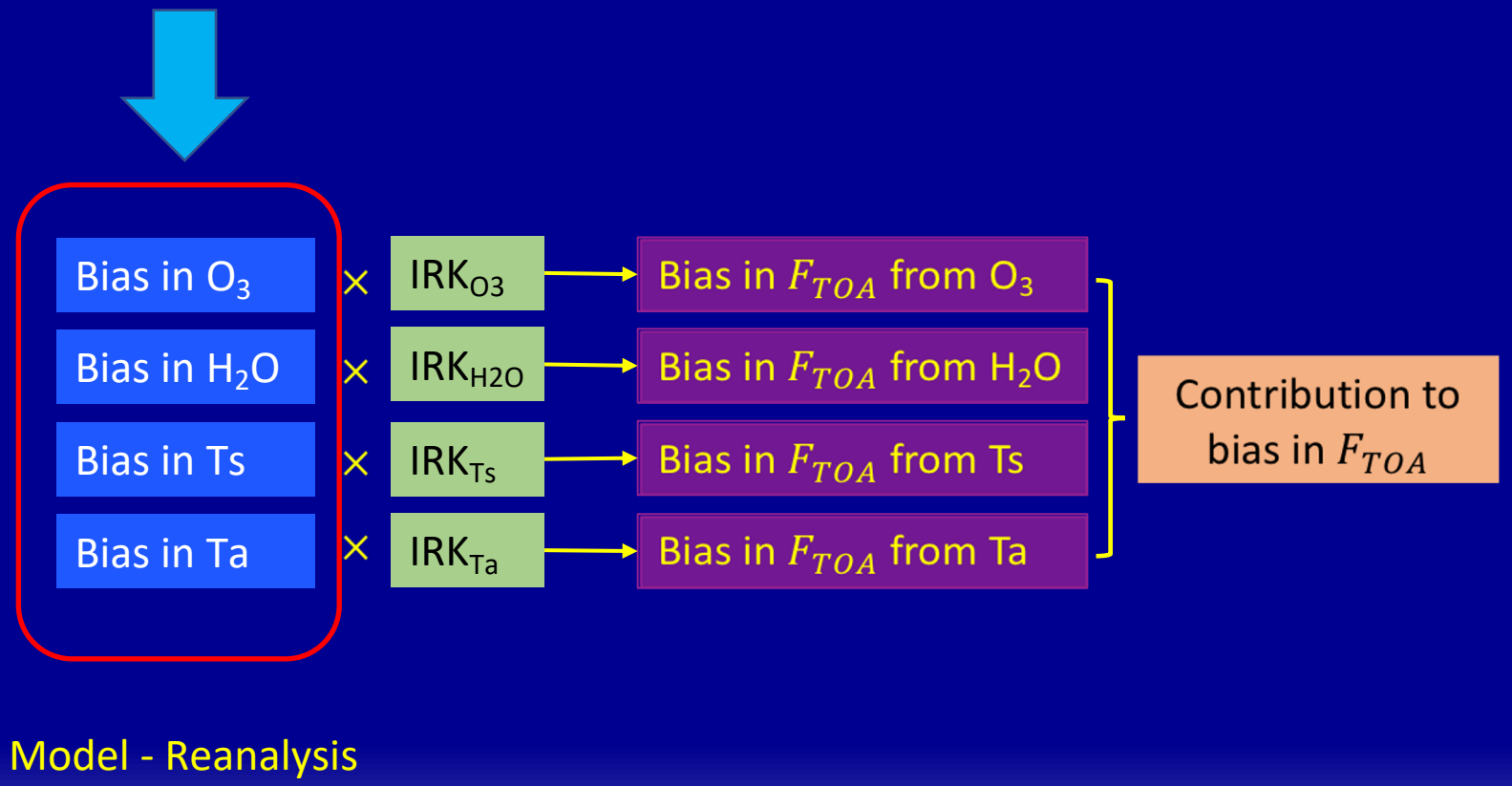

Model - Reanalysis

O_3 bias to reanalysis

O_3 IRK

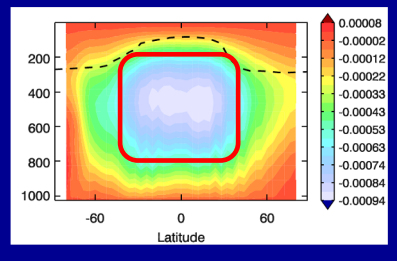

- Dominant region: 200-800 hPa, 45S - 45N
- GEOCCM, CMAM, and CESM have similar patterns
  - Low-high pattern
  - ⇒ small biases in TOA fluxes
- 2 EMAC and MRI-ESM1r1
  - all overestimate
  - ⇒ large flux biased in low latitudes
- SOCOL3
  - strongest overestimates (>20 ppb) in NH
  - ⇒ Large flux bias in NH subtropical
- MRI-ESM1r1:
  - large positive bias over tropical upper troposphere
  - add additional bias in tropics
  - ⇒ Largest tropical flux bias (-0.4 W/m^2)

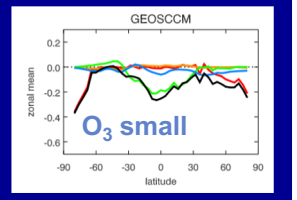

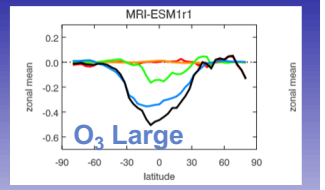

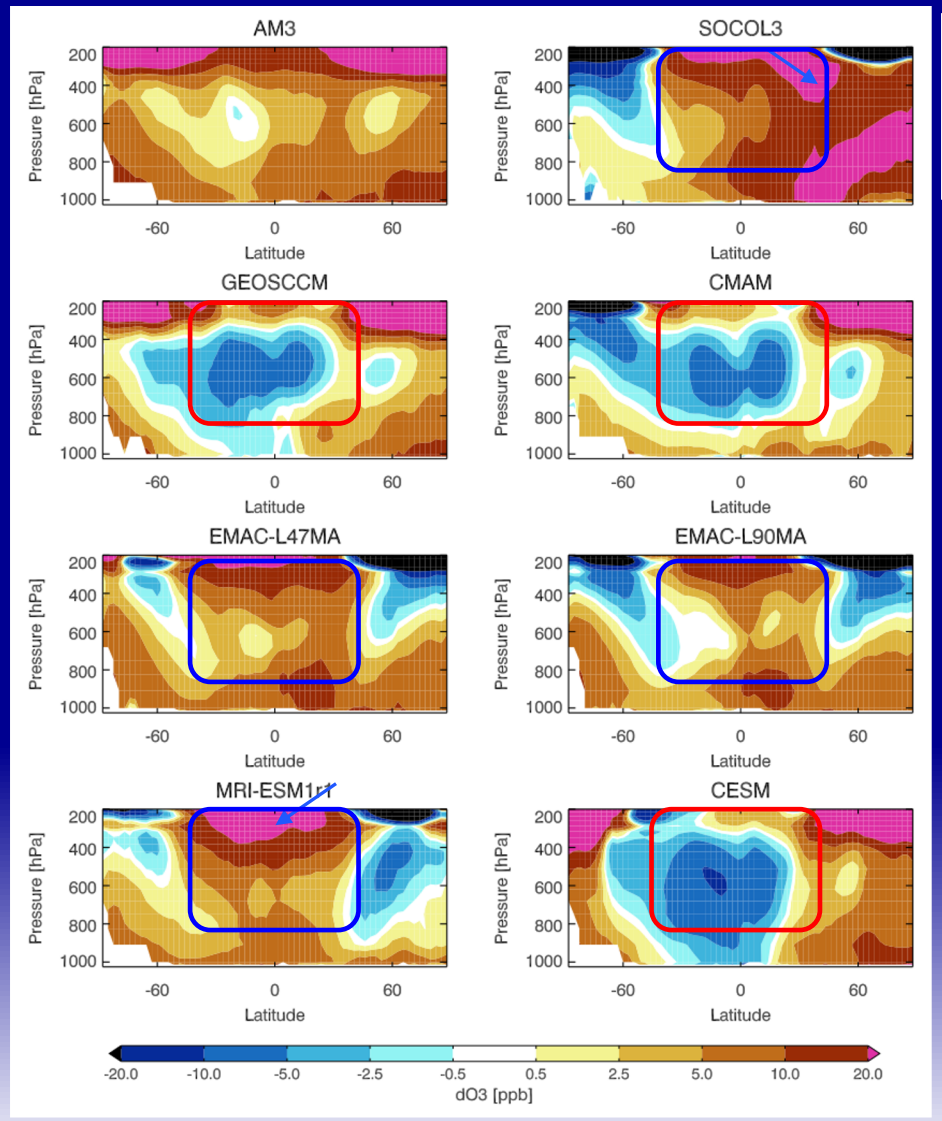

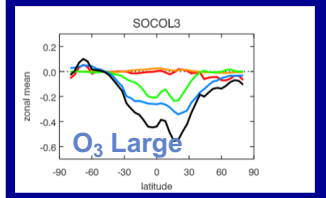

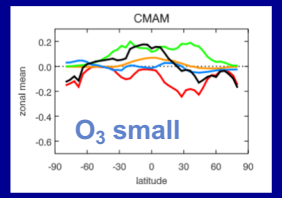

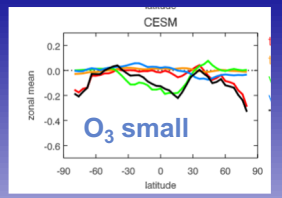

H_2O bias to reanalysis

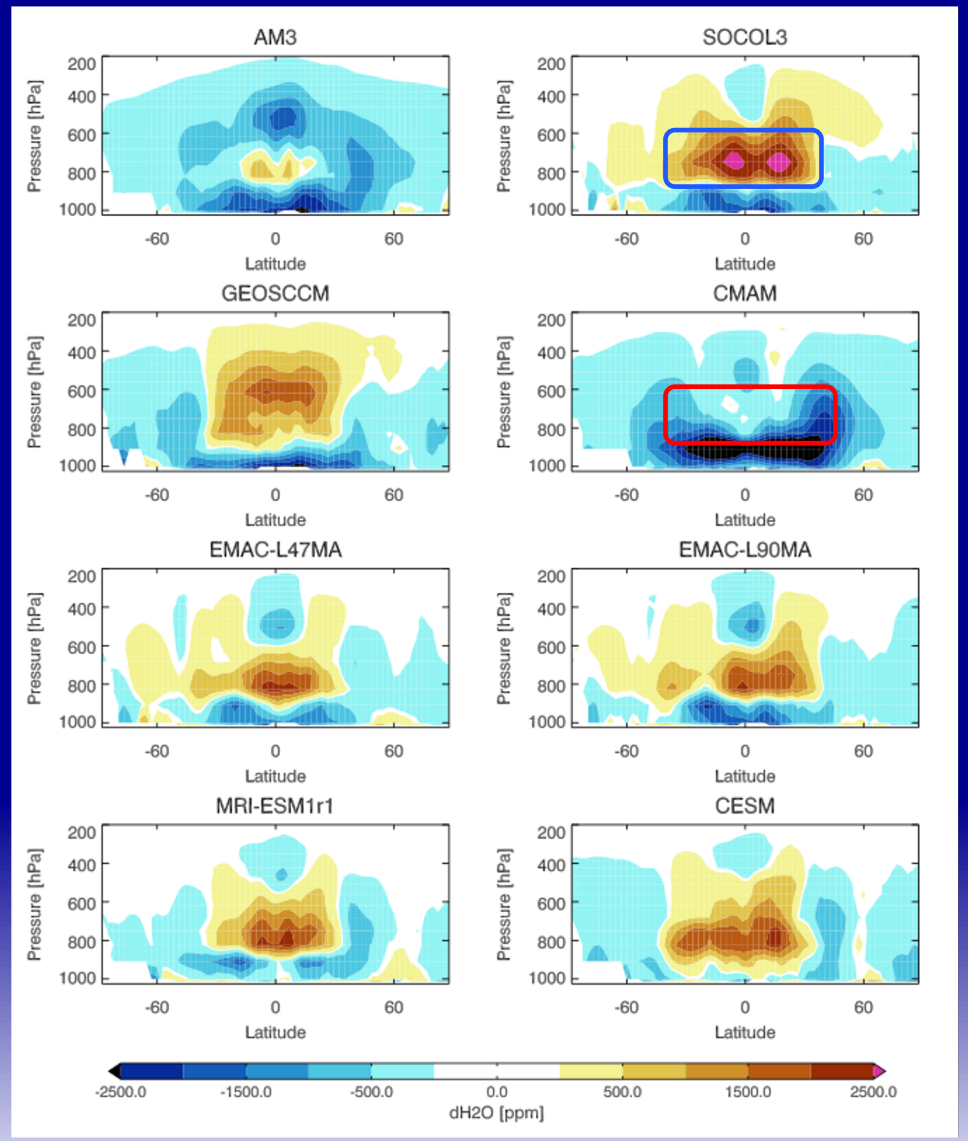

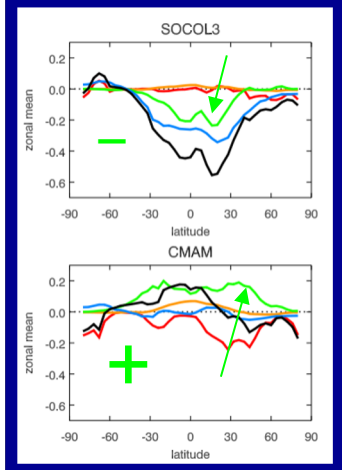

- Dominant region:
  - 900 - 600 hPa, 30S – 30N
  - tropical and lower/middle troposphere region ⇒ Large TOA flux bias
- SOCOL3:
  - strongest positive bias
  - tropical 800~600 hPa
  - ⇒ negative TOA flux bias
- CMAM:
  - strongest negative bias
  - ⇒ positive TOA flux bias

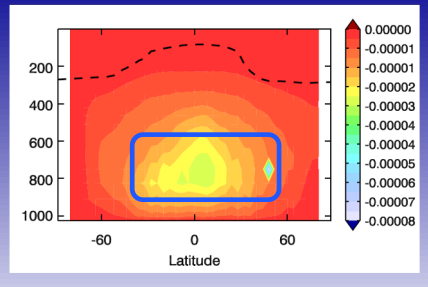

H_2O IRK

Ts bias to reanalysis

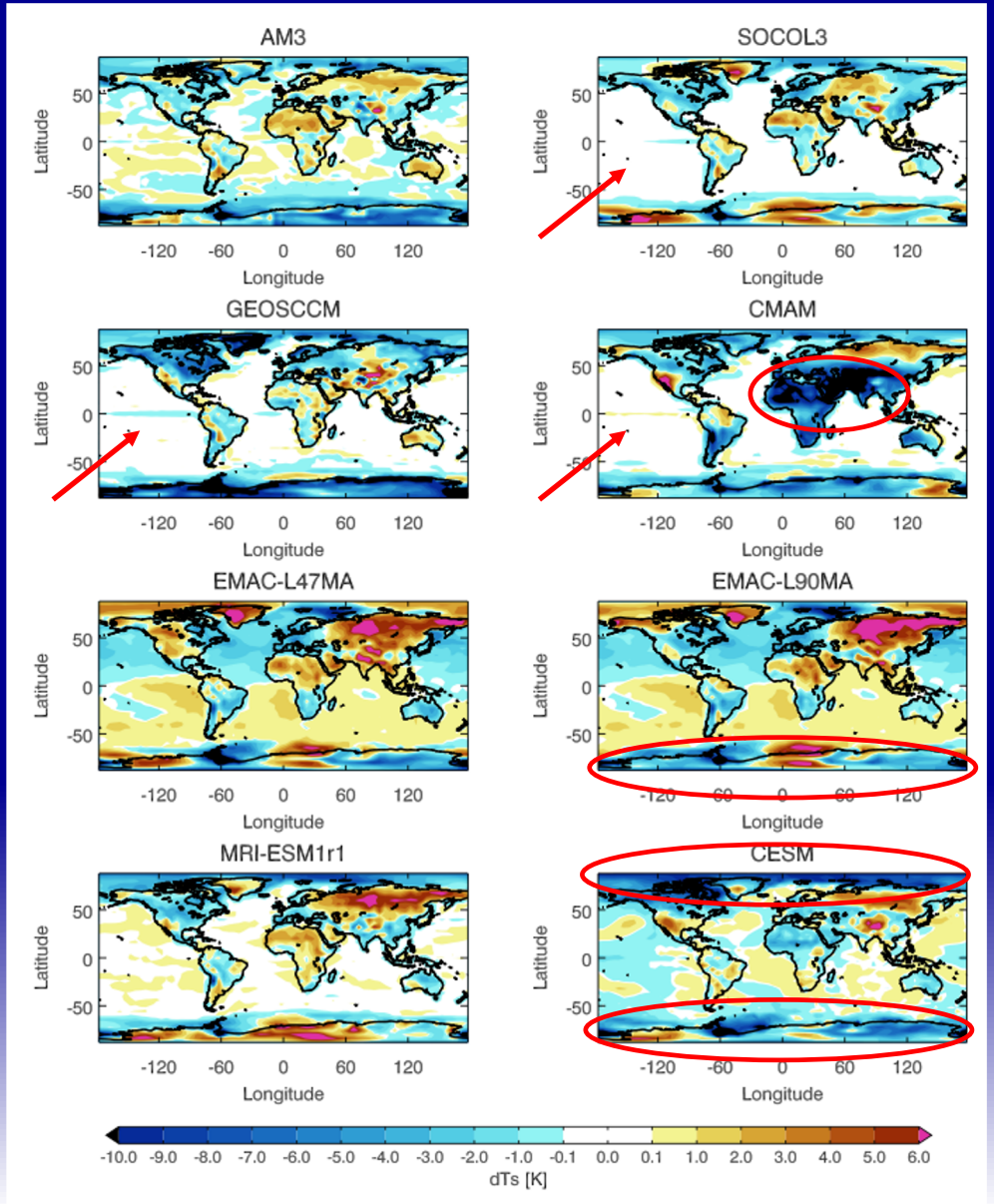

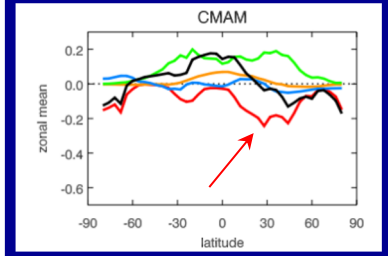

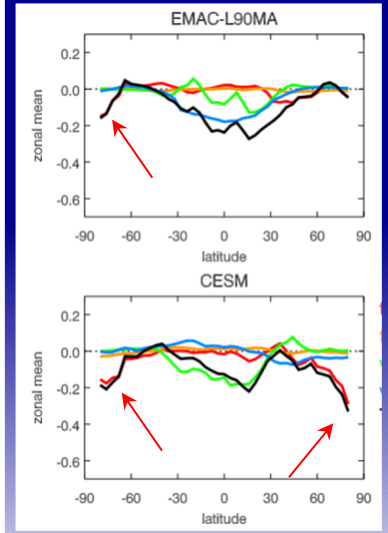

- Localized bias ⇒ cancellation
- SOCOL3, GEOSCCM, CMAM:
  - Small differences in global SST
  - Except polar sea.
- Large differences over land, e.g.
  - CMAM at Middle East and N. Africa, ⇒ flux bias
- AM3, GEOSCCM, CMAM, two EMAC, CESM:
  - Zonally constantly underestimate at polar region ⇒ flux bias

Ta bias to reanalysis

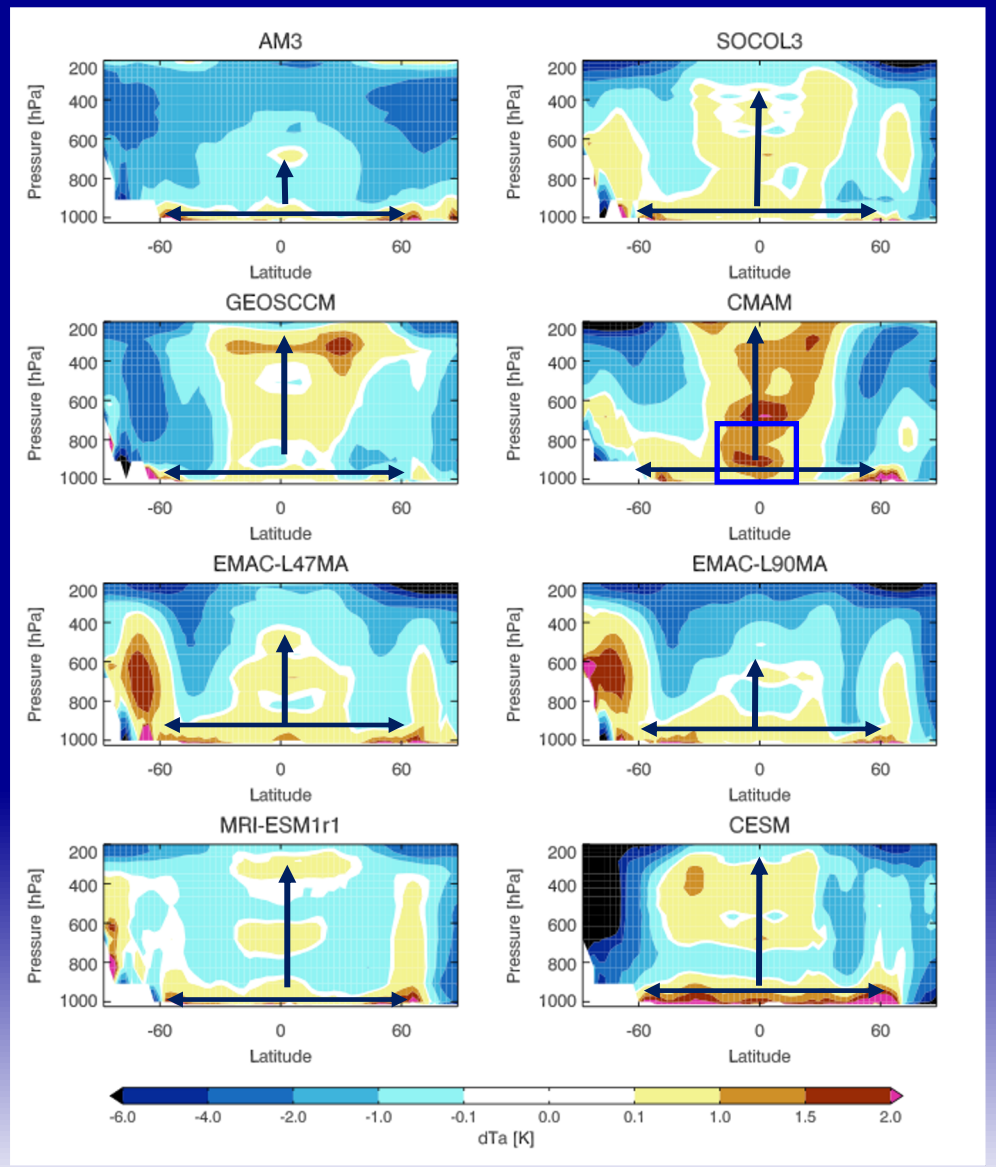

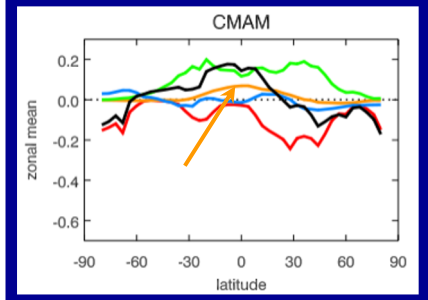

T_a IRK

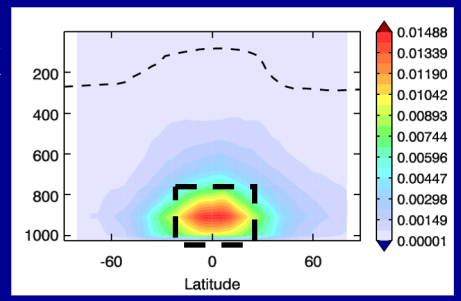

- Symmetric about equator
- Lower troposphere
  - all model overestimate Ta.
- CMAM:
  - overestimate Ta
  - tropics entire troposphere
  - strong at lower troposphere
  - ⇒ flux bias in tropics
- Not contribute much to flux bias in other models

Conclusions

- **We demonstrate a method to benchmark the model TOA fluxes with the 9.6-μm O_3 band satellite observations**
  - Where and which variables in the model bias ➔ flux bias
  - Most model atmosphere: more opaque than reanalysis atmosphere
  - Except CMAM in tropics is more transparent.
  - AM3: smallest flux bias but right for wrong reason.
  - SOCOL3 and MRI-ESM1r1 have large potential to improve their fluxes.
  - Both ozone and water vapor contribute more biases to fluxes than temperature
- **Adding AIRS/CrIS IRK products will enforce the capability of climate models.**
- **The similar study could be applied to any other GHG, i.e. CO_2 and CH_4.**

Acknowledge:

IGAC/SPARC Chemistry-Climate Model Initiative COMMITTEE

Kevin W. Bowman[2], Helen Worden[3], Kazu. Miyazaki[4] Andrew Conley[3], Jean-Fraçois Lamarque[3], Fabien Paulot[5], David Paynter[5], Luke Oman[6], Sarah Strode[6], Eugene Rozanov [7,8], Andrea Stenke[8], Laura Revell[9], David Plummer[10], Makoto Deushi[11], Kiyotaka Shibata[11], Patrick Jöckel[12], Markus Kunze[13]

1. University of California, Los Angeles, USA; 2. Jet Propulsion Laboratory, Caltech, USA; 3. National Center for Atmospheric Research, USA; 4. Japan Agency for Marine-Earth Science and Technology, Japan; 5. NOAA, Geophysical Fluid Dynamics Laboratory, USA; 6. NASA Goddard Space Flight Center, USA; 7. Physikalisch-Meteorologisches Observatorium Davos– World Radiation Center (PMOD/WRC), Davos, Switzerland; 8. Institute for Atmospheric and Climate Science, ETH Zürich (ETHZ), Zürich, Switzerland; 9. Bodeker Scientific, Christchurch, New Zealand; 10. Environment Canada, Canada; 11. Meteorological Research Institute, Japan; 12. German Aerospace Center (DLR), Germany; 13. Freie Universität Berlin, Berlin, Germany

Funded by NASA ROSES AuraST

Thank you!

Clear sky

Bias in O_3	×	IRK_{O3}	→ Bias in F_{TOA} from O_3	Contribution to bias in F_{TOA}
Bias in H_2O	×	IRK_{H2O}	→ Bias in F_{TOA} from H_2O	
Bias in Ts	×	IRK_{Ts}	→ Bias in F_{TOA} from Ts	
Bias in Ta	×	IRK_{Ta}	→ Bias in F_{TOA} from Ta	

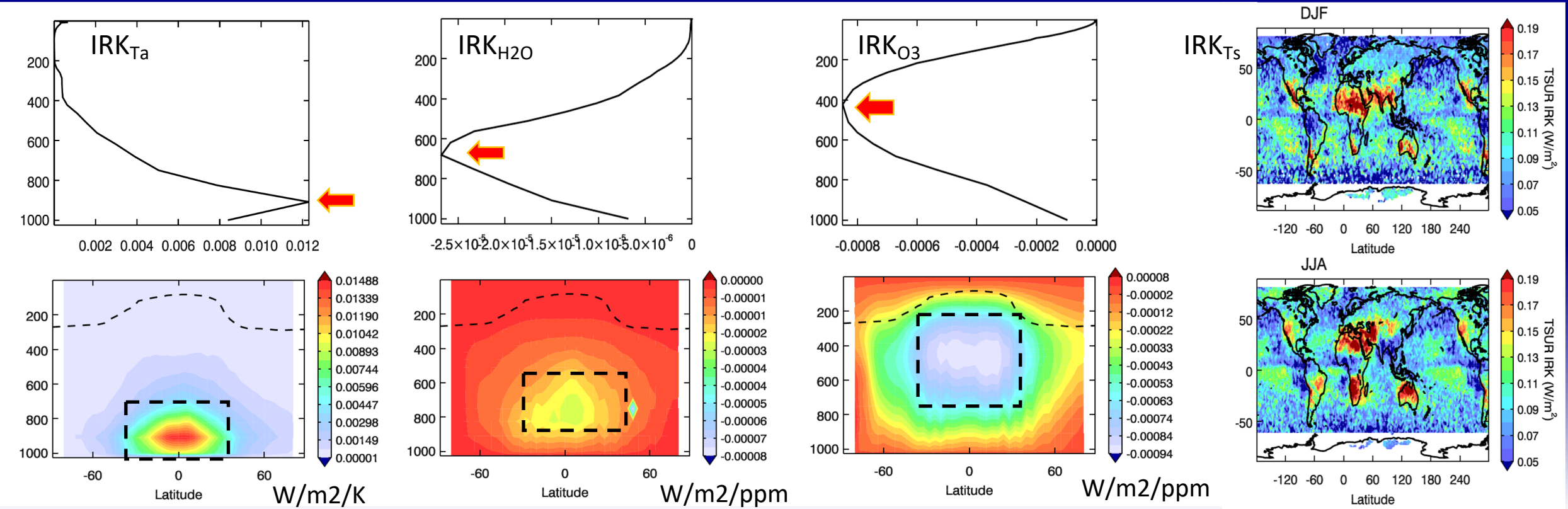

Benchmarking 9.6-µm ozone band top-of-atmosphere (TOA) flux in chemistry-climate models using satellite instantaneous radiative kernels (IRK) products

Le Kuai [1,2], Kevin W. Bowman[2], Helen Worden[3], Kazu. Miyazaki[4] , Andrew Conley[3], Jean-Fraçois Lamarque[3], Fabien Paulot[5], David Paynter[5], Luke Oman[6], Sarah Strode[6], Eugene Rozanov [7,8], Andrea Stenke[8], Laura Revell[9], David Plummer[10], Makoto Deushi[11], Kiyotaka Shibata[11], Patrick Jöckel[12], Markus Kunze[13]

1. University of California, Los Angeles, USA; 2. Jet Propulsion Laboratory, Caltech, USA; 3. National Center for Atmospheric Research, USA; 4. Japan Agency for Marine-Earth Science and Technology, Japan; 5. NOAA, Geophysical Fluid Dynamics Laboratory, USA; 6. NASA Goddard Space Flight Center, USA; 7. Physikalisch-Meteorologisches Observatorium Davos– World Radiation Center (PMOD/WRC), Davos, Switzerland; 8. Institute for Atmospheric and Climate Science, ETH Zürich (ETHZ), Zürich, Switzerland; 9. Bodeker Scientific, Christchurch, New Zealand; 10. Environment Canada, Canada; 11. Meteorological Research Institute, Japan; 12. German Aerospace Center (DLR), Germany; 13. Freie Universität Berlin, Berlin, Germany

1	ACCESS	ACCESS-CCM	refC1	r1i1p1	v1	mon	mon	mon		mon
2	CCCma	CMAM								
3	CHASER-MIROC-ESM	CHASER-MIROC-ESM	refC1sd	r1i1p1	v1	mon	mon	mon		
4	CNRM-CERFACS	CNRM-CM5-3	refC1	r1i1p0-2	v1	day	day	day	day	
5	CNRM-CERFACS	MOCAGE	refC1			mon	mon	mon		
6	ETH-PMOD	SOCOL3	refC1	r1i1p1	v1	day/mon	day/mon	day/mon	day	mon
7	GSFC	GEOSCCM	refC1	r1i1p1	v1	day	day	day	day	
8	IPSL	IPSL	refC1			day	day	day	day	
9	MESSy	EMAC-L47MA								
10	MESSy	EMAC-L90MA								
11	MOHC	HadGEM3	refC1	r1i1p1	v1	day/mon	mon	day/mon		mon
12	MRI	MRI-ESM1r1	refC1	r1i1p1	v1	day	day	day	day	
13	NIES	CCSRNIES-MIROC3.2	refC1	r1i1p1	v1	day	day	day	day	
14	NIWA	NIWA-UKCA	refC1	r1i1p1	v1	day/mon		day/mon		mon
15	U-CAMBRIDGE	UMUKCA-UCAM	refC1/C1sd	r1i1p1	v1	mon	mon	mon		
16	U-LAQUILA	ULAQ-CCM	refC1	r1i1p1	v1	mon	mon	mon		
17	U-LEEDS	SLIMCAT	refC1sd	r1i1p1	v1			mon		
18	U-LEEDS	UMSLIMCAT	refC1	r1i1p1	v1	mon	mon	mon	day	
19	GFDL/NOAA	AM3								
20	NCAR	CESM								

Model improvement advises:

- GEOSCCM, CMAM and CESM are three models that ozone is not the major source of flux bias. However
  - GEOSCCM can improve its surface temperature at polar region
  - CMAM can better estimate 1) their surface temperature at subtropical major continents and 2) water vapor at subtropical lower troposphere to reduce their bias in TOA fluxes.
- Other models need to improve their mid-upper tropospheric ozone over tropics and subtropics. SOCOL3 also needs better simulate NH ozone.
- AM3 and CMAM simulates mid and upper tropospheric water vapor better than other models but has stronger underestimates of lower tropospheric water vapor over low latitudes than other models and has potential to improve.
- Other models need to estimate less mid tropospheric water vapor while more lower tropospheric water vapor.

Model	Suggestions
AM3	H2O: tropical and subtropical lower troposphere, (good for mid troposphere) O3: Low latitude region mid-upper troposphere Ts: Africa and India
SOCOL3	O3: Low latitude region and northern hemisphere mid-upper troposphere Ts: Greenland, Africa and India H2O:dipole in low latitude
GESCCM	Ts: Antarctic, polar region H2O: troposphere 30N~30S
CMAM	H2O:tropical and subtropical lower troposphere, (good for mid troposphere) Ts: major continents, especially Africa, Europe and south and mid Asia, and Australia
EMAC-L47MA	O3: Low latitude region mid-upper troposphere Ts: Russian, Greenland, Alaska and west Canada, as well as Africa and Middle East H2O: dipole in low latitude
EMAC-L90MA	O3: Low latitude region mid-upper troposphere Ts: Russian, Greenland, Alaska and west Canada, as well as Africa and Middle East H2O: dipole in low latitude
MRI-ESM1r1	O3: Low latitude region mid-upper troposphere Ts: Russian, Greenland, Alaska and west Canada, as well as Africa and Middle East H2O: dipole in low latitude

APPLICATION 2:
Hydrological controls on the tropospheric ozone greenhouse gas effect (Kuai et al., 2017)

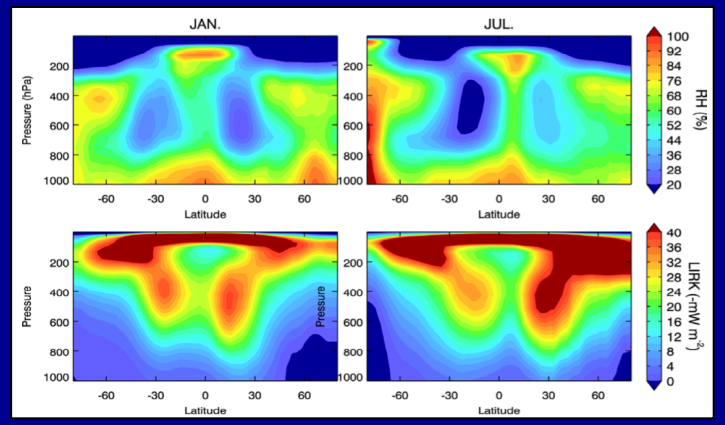

- Significant anti-correlation between RH and O_3 IRK
- Lead to climate feedbacks in O3 forcing
- Through changes in Ts and water vapor

$$RH = \frac{e_w(H_2O,P)}{e_w^*(T,P)}$$

2nd order effect

$$\Delta F_{TOA} = \frac{\partial F_{TOA}}{\partial O_3}\Delta O_3 + \frac{\partial F_{TOA}}{\partial T_{sur}}\Delta T_{sur} + \frac{\partial F_{TOA}}{\partial T_{atm}}\Delta T_{atm} + \frac{\partial F_{TOA}}{\partial H_2O}\Delta H_2O + r_s$$

9.6 µm band flux change | O_3 | Surface temperature | Atmos. temperature | Water vapor | residual

APPLICATION: TOA flux bias attribution

$$\underbrace{\Delta F_{TOA}}_{\text{9.6 µm band flux change}} = \underbrace{\frac{\partial F_{TOA}}{\partial O_3}\Delta O_3}_{O_3} + \underbrace{\frac{\partial F_{TOA}}{\partial T_{sur}}\Delta T_{sur}}_{\text{Surface temperature}} + \underbrace{\frac{\partial F_{TOA}}{\partial T_{atm}}\Delta T_{atm}}_{\text{Atmos. temperature}} + \underbrace{\frac{\partial F_{TOA}}{\partial H_2O}\Delta H_2O}_{\text{Water vapor}} + \underbrace{r_s}_{\text{residual}}$$

Clear sky

Bias in O_3	×	IRK_{O3}	→ Bias in F_{TOA} from O_3	Contribution to bias in F_{TOA}
Bias in H_2O	×	IRK_{H2O}	→ Bias in F_{TOA} from H_2O	
Bias in Ts	×	IRK_{Ts}	→ Bias in F_{TOA} from Ts	
Bias in Ta	×	IRK_{Ta}	→ Bias in F_{TOA} from Ta	